AMERICAN SOCIETY FOR MICROBIOLOGY | Journal of Virology®

PATHOGENESIS AND IMMUNITY

Peroxiredoxin 1 Interacts with TBK1/IKKε and Negatively Regulates Pseudorabies Virus Propagation by Promoting Innate Immunity

Lin Lv,[a] Juan Bai,[a] Yanni Gao,[a] Ling Jin,[b] Xianwei Wang,[a] Mingzhu Cao,[a] Xing Liu,[a] Ping Jiang[a,c]

[a]Key Laboratory of Animal Diseases Diagnostic and Immunology, Ministry of Agriculture, MOE International Joint Collaborative Research Laboratory for Animal Health and Food Safety, College of Veterinary Medicine, Nanjing Agricultural University, Nanjing, China

[b]Department of Biomedical Sciences, College of Veterinary Medicine, Oregon State University, Corvallis, Oregon, USA

[c]Jiangsu Co-Innovation Center for Prevention and Control of Important Animal Infectious Diseases and Zoonoses, Yangzhou, China

ABSTRACT Peroxiredoxin 1 (PRDX1) is a cellular antioxidant enzyme that is crucial for diverse fundamental biological processes, such as autophagy, inflammation, and carcinogenesis. However, molecular mechanisms underpinning its diverse roles are not well understood. Here, we report that PRDX1 positively regulates interferon (IFN) induction and that pseudorabies virus (PRV) targets PRDX1 to evade IFN induction. PRV UL13 encodes a serine/threonine kinase important for PRV infection, although its biological function remains obscure. We identified PRDX1 as a UL13-interacting protein. Virological and biochemical assays demonstrate that PRDX1 promotes IFN induction by interacting with TANK-binding kinase 1 (TBK1) and IκB kinase ε (IKKε). Conversely, UL13 accelerates PRDX1 degradation via the ubiquitin-proteosome pathway in a kinase-dependent manner. In doing so, PRV inhibits IFN induction during productive infection, which requires PRDX1 expression. This study uncovers an essential role of PRDX1 in the innate immune response and reveals a new viral immune evasion strategy to counteract cellular defenses.

IMPORTANCE PRV interacts with numerous cellular proteins during productive infection. Here, we demonstrated the interaction of viral protein UL13 with the antioxidant enzyme PRDX1, which functions in multiple signal transduction pathways. We found that PRDX1 participates in the type I IFN pathway by interacting with TBK1 and IKKε, thereby negatively regulating PRV propagation. However, UL13 ubiquitinates PRDX1, which routes PRDX1 into proteasomes for degradation and effectively reduces its expression. These results illuminate the fundamental role that PRDX1 plays in the IFN pathway, and they identify a potential target for the control of PRV infection.

KEYWORDS PRDX1, PRV, UL13, TBK1, IKKε, innate immunity

Pseudorabies virus (PRV), a large DNA virus that can convert between latent and lytic cycles, causes neuroencephalitis, respiratory disease, and reproductive failure (1–4). The genome of PRV is largely colinear with the genomes of herpes simplex virus 1 (HSV-1) and other alphaherpesviruses. Alphaherpesviruses encode 8 capsid proteins, 23 tegument proteins, and 14 envelope proteins. The tegument is located between the capsid and the envelope and has a variety of functions, including viral entry, secondary envelopment, viral capsid nuclear transportation during infection, and immune evasion. UL13, one of the tegument proteins, is characterized as a serine/threonine protein kinase, and the protein kinase site of UL13 is conserved throughout the alphaherpesvirus subfamily (these enzymes are collectively known as the conserved herpesvirus protein kinases [CHPKs]) (5, 6). HSV-1 UL13 can modulate the modification of viral proteins VP11/12, ICP22, ICP0, UL41, and UL49 (7–10). In addition, PRV UL13 cooperates with US3 to facilitate transport of viral capsids to the distal axon (11). Similarly, the

Citation Lv L, Bai J, Gao Y, Jin L, Wang X, Cao M, Liu X, Jiang P. 2021. Peroxiredoxin 1 interacts with TBK1/IKKε and negatively regulates pseudorabies virus propagation by promoting innate immunity. J Virol 95:e00923-21. https://doi.org/10.1128/JVI.00923-21.

Editor Jae U. Jung, Lerner Research Institute, Cleveland Clinic

Address correspondence to Xing Liu, xingliu@njau.edu.cn, or Ping Jiang, jiangp@njau.edu.cn.

Received 7 June 2021
Accepted 6 July 2021
Accepted manuscript posted online 14 July 2021
Published 9 September 2021

UL13 gene product encoded by HSV-2 is required to mediate viral replication and pathogenesis *in vitro* and *in vivo* (12). Recent studies demonstrate that PRV UL13 antagonizes innate immunity by inhibiting the beta interferon (IFN-β) signaling pathway (13, 14), although the precise mechanism needs to be investigated further.

The innate immune system activates robust antiviral responses as the first line of defense against viral infection when it recognizes pathogen-associated molecular patterns (PAMPs) (15, 16). Upon DNA virus infection, viral components are recognized by intracellular DNA sensors (cyclic GAMP synthase [cGAS]) (17), IFN-inducible protein 16 (IFI16) (18), and DEAD box helicase 41 (DDX41) (19). The surveillance system then activates the stimulator of IFN genes (STING), which recruits IκB kinase ε (IKKε) and TANK-binding kinase 1 (TBK1) and promotes the phosphorylation of downstream IFN regulatory factor 3 (IRF3), leading to the production of IFN-β and IFN-stimulated genes (ISGs) (20–22). TBK1 and IKKε play pivotal roles in mediating IRF3 phosphorylation and activation, and their activities are crucial for maintaining immune homeostasis (23). Recently, many factors that positively or negatively regulate type I IFN production by manipulating the TBK1/IKKε complex in various ways have been identified. For example, GSK3b positively regulates self-association and autophosphorylation of TBK1, promoting type I IFN production (24). TRIM26 and ubiquitin-specific protease 38 (USP38) can link TBK1 to NF-κB essential modulator (NEMO) and mediate the activation of TBK1 (25, 26). The E3 ligases Nrdp1, Mib1, Mib2, and RNF128 promote K63-linked polyubiquitination of TBK1 to activate it and to stimulate IFN production (27–29). Conversely, the E3 ligase TRIM27, deltex-4 (DTX4), and TRAF-interacting protein (TRIP) facilitate K48-linked polyubiquitination of TBK1, tagging it for proteasome-dependent degradation (30–32). Protein phosphatase 1B (PPM1B) dephosphorylates TBK1 at serine 172 to inhibit TBK1-mediated IRF3 phosphorylation (33). Suppressor of IκB kinase ε (SIKE) blocks IFN production by disrupting the interaction of IKKε or TBK1 with IRF3 (34). Finally, the DExD/H-box RNA helicase 19 (DDX19) inhibits type I IFN production by disrupting TBK1-IKKε-IRF3 interactions (35).

In this study, peroxiredoxin 1 (PRDX1), an antioxidant enzyme, was found in a mass spectrometry-based screen to associate with PRV-encoded protein kinase UL13. PRDX1 negatively regulates PRV propagation by enhancing TBK1/IKKε-mediated IFN-β signaling. However, UL13 tags PRDX1 for degradation in proteasomes via K48-linked ubiquitination. As a consequence, deletion of UL13 or introduction of the serine/threonine mutation K93A into UL13 reduces viral replication in PRDX1$^{+/+}$ cell lines, but this effect is absent in PRDX1$^{-/-}$ cell lines. Our results reveal the molecular mechanism by which UL13 targets PRDX1 to antagonize the IFN-β signaling pathway.

RESULTS

Cellular PRDX1 is a target of the PRV UL13 protein. To explore the function of PRV UL13, we used electrospray ionization mass spectrometry (ESI-MS) to identify host proteins that potentially interact with UL13. Seven candidates were found in the screen (Fig. 1A) and were selected for analysis. The corresponding genes were cloned into the pCDNA3.1-Myc mammalian expression vector. Coimmunoprecipitation (Co-IP) assays using HEK293T cells transfected with the pCDNA3.1-Myc constructs and UL13-Flag showed that only PRDX1 interacted with UL13 (Fig. 1B). Endogenous PRDX1 protein in HEK293T cells also interacted with UL13 during PRV infection (Fig. 1C). These results suggest that PRDX1 is a specific host factor targeted by the PRV UL13 protein.

PRDX1 downregulates PRV replication. To investigate the role of PRDX1 in PRV replication, PRDX1 knockout (PRDX1$^{-/-}$) HEK293T and PK-15 cells were constructed using the CRISPR/Cas9 or lentiCRISPRv2 systems and verified by Western blotting (see Fig. S1 in the supplemental material). The modified cells were then infected with PRV ZJ01, recombinant ZJ01 containing a UL13 deletion (ΔUL13), or the corresponding rescued virus (ΔUL13R). These were constructed using CRISPR/Cas9 and verified as shown in Fig. S2. The results showed that ZJ01, ΔUL13, and ΔUL13R replication levels in PRDX1$^{-/-}$ HEK293T cells were increased, compared to levels in wild-type and PRDX1$^{-/-}$ rescued cells. Intriguingly, ΔUL13 growth was largely restored in PRDX1$^{-/-}$ HEK293T cells (Fig. 2A). Note that the viability of PRDX1$^{+/+}$, PRDX1$^{-/-}$, and PRDX1$^{-/-}$ rescued cells was

A

Protein	Accession	Protein Discription	Coverage PCDH	Coverage UL13-Flag	# Peptides PCDH	# Peptides UL13-Flag
PRDX1	A0A3L7I4D2	peroxiredoxin 1	2.46	30.00	1	10
C1BPQ	A0A1U7QHB5	complement component 1 Q subcomponent-binding protein	-	24.91	-	3
RPS18	D2Y5X1	Ribosomal protein S18	1.04	23.62	1	3
ANXA2	C0HJG9	Annexin A2	-	21.35	-	1
HNRNP A2B1	A0A3Q0CCM9	heterogeneous nuclear ribonucl eoproteins A2/B1	-	17.78	-	2
TIMM10	A0A1A6HWL3	translocase of inner mitochond rial membrane 10	-	17.74	-	4
ARG1	G3IE79	arginase 1	-	17.43	-	1

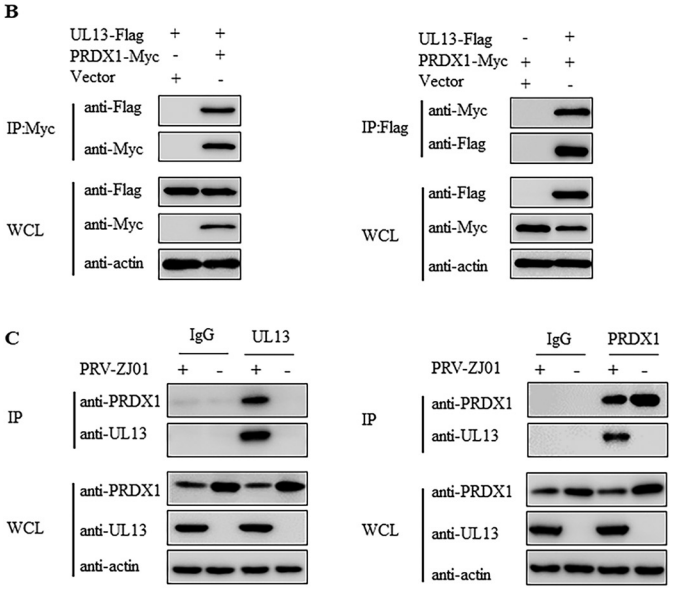

FIG 1 PRV UL13-binding proteins detected by mass spectrometry. (A) PRV UL13-binding proteins were detected using ESI-MS. HEK293T cells were transfected with a UL13-Flag construct (3 μg) or with empty vector (pCDH) and incubated for 30 h. Cells were collected, and immunoprecipitation (IP) products were probed using ESI-MS to identify candidate binding proteins. Coverage indicates the percentage of protein sequence sampled as identified peptides. Peptides are the number of distinct peptide sequences associated with the protein. (B) To confirm the association between UL13 and PRDX1, HEK293T cells were transfected with PRDX1-Myc (3 μg) along with UL13-Flag (3 μg) or empty vector. Thirty hours after transfection, cells were harvested and subjected to immunoprecipitation assays using the indicated antibodies. Precipitated samples and whole-cell lysates (WCL) were probed with antibodies against Flag, Myc, and β-actin. The results shown are representative of three independent experiments. (C) HEK293T cells were infected with PRV ZJ01 (MOI of 0.1). Twelve hours after infection, cells were harvested and subjected to immunoprecipitation assays using the indicated antibodies (anti-PRDX1, 1 μg/ml; anti-UL13, 1 μg/ml).

indistinguishable (Fig. 2B). Similar results were obtained in PRDX1$^{+/+}$, PRDX1$^{-/-}$, and PRDX1$^{-/-}$ rescued PK-15 cells (Fig. 2C and D). These data demonstrate that PRDX1 plays an important role in PRV replication.

PRDX1 potentiates antiviral immunity. To evaluate whether PRDX1 plays a role in IFN induction by cGAS/STING, we transfected PRDX1$^{+/+}$, PRDX1$^{-/-}$, and PRDX1$^{-/-}$ rescued HEK293T and PK-15 cells with poly(dA-dT) or cGAS-Flag and STING-Flag. Twenty-four hours after transfection, total RNA was extracted and analyzed using quantitative real-time RT-PCR (qRT-PCR) to quantitate IFN-β. The results showed that IFN-β mRNA levels in the PRDX1$^{-/-}$ cells were significantly lower than those in wild-type and PRDX1$^{-/-}$ rescued cells (Fig. 3A and B).

To evaluate the role of PRDX1 in IFN induction during PRV infection, PRDX1$^{+/+}$, PRDX1$^{-/-}$, and PRDX1$^{-/-}$ rescued HEK293T and PK-15 cells were infected with PRV ZJ01, ΔUL13, or ΔUL13R. qRT-PCR analyses revealed that IFN-β, ISG15, and ISG56

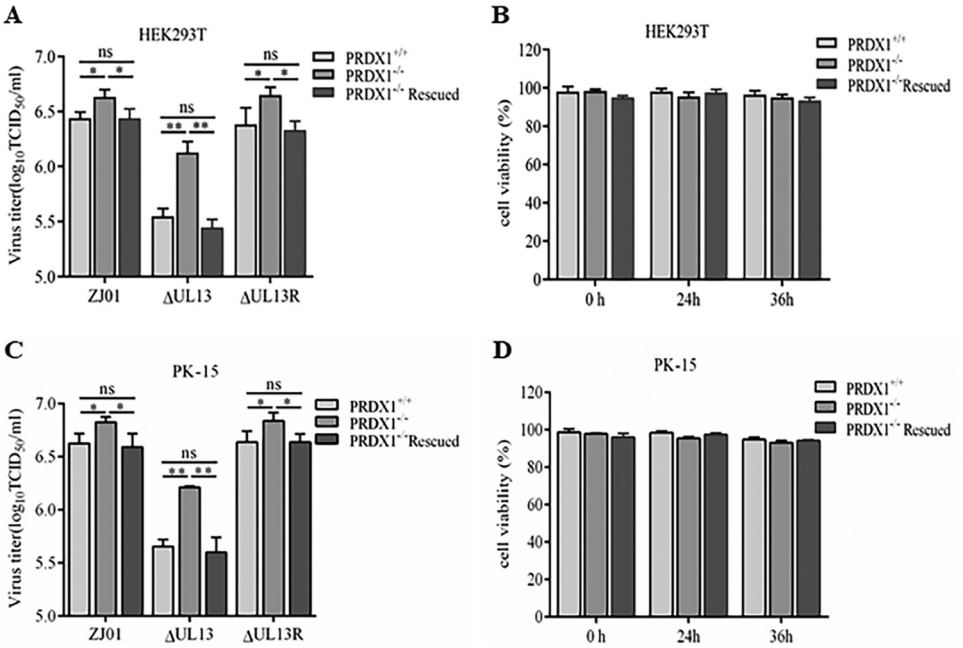

FIG 2 PRDX1 downregulates PRV replication. (A) PRV replication in PRDX1$^{+/+}$, PRDX1$^{-/-}$, and PRDX1$^{-/-}$ rescued HEK293T cells. Cells were infected with PRV ZJ01, recombinant ZJ01 containing a UL13 deletion (ΔUL13), or the corresponding rescued virus (ΔUL13R) at an MOI of 0.01. Twenty-four hours after infection, cells were harvested and total virus yields were determined using the designated cells. Virus yields are shown as the 50% tissue culture infective dose ($TCID_{50}$) per milliliter. (B) Viability assays of PRDX1$^{+/+}$, PRDX1$^{-/-}$, and PRDX1$^{-/-}$ rescued HEK293T cells. A total of 10^4 cells were seeded into 96-well plates, and viability was measured using a cell counting kit 8 (Beyotime) at 0 h, 24 h, and 36 h. (C) PRV replication in PRDX1$^{+/+}$, PRDX1$^{-/-}$, and PRDX1$^{-/-}$ rescued PK-15 cells. (D) Viability assay results for PRDX1$^{+/+}$, PRDX1$^{-/-}$ and PRDX1$^{-/-}$ rescued PK-15 cells. Methods were identical to those used in panels A and B. The results shown are representative of three independent experiments. Differences were assessed using multiple comparison analysis. *, $P < 0.05$; **, $P<0.01$.

mRNA levels in PRDX1$^{-/-}$ HEK293T cells were significantly lower after infection than those in wild-type or PRDX1$^{-/-}$ rescued cells. In addition, the ΔUL13 mutant induced higher levels of innate immunity, compared to wild-type ZJ01 or ΔUL13R (Fig. 3C). Similar results were obtained in PRDX1$^{+/+}$, PRDX1$^{-/-}$, and PRDX1$^{-/-}$ rescued PK-15 cells (Fig. 3D). These results suggest that PRDX1 plays an important role in UL13-mediated innate immunity.

PRDX1 positively regulates IFN-β signaling via interactions with TBK1 and IKKε. To analyze interactions between PRDX1 and other proteins more closely, HEK293T cells were transfected with PRDX1, TBK1, and IKKε expression vectors. Co-IP analysis showed that PRDX1 interacted with IKKε and TBK1 (Fig. 4A and B) but not with cGAS and STING (see Fig. S3A and B). The Co-IP results also showed that endogenous PRDX1 interacted with IKKε and TBK1 (Fig. 4C and D). To investigate how PRDX1 functions in IKKε- and TBK1-mediated type I IFN production, we conducted experiments to examine how PRDX1 affects IFN-β promoter activation mediated by IKKε and TBK1. The results showed that ectopically expressed PRDX1 strongly enhanced IFN-β reporter activation induced by IKKε and TBK1, in a dose-dependent manner (Fig. 4E and F). Consistent with these results, IFN-β mRNA levels induced by IKKε and TBK1 were equally enhanced by PRDX1 (Fig. 4G and H).

To definitively confirm the function of PRDX1 in the PRV-induced type I IFN response, key factors in the type I IFN pathway (cGAS, STING, pTBK1, TBK1, IKKε, pIRF3, and IRF3) were detected by Western blotting after virus infection. As shown in Fig. 4I, ΔUL13 clearly increased phosphorylation of TBK1 and IRF3, compared to wild-type and ΔUL13R viruses. In PRDX1$^{-/-}$ HEK293T or PK-15 cells, however, virus infection decreased TBK1 and IRF3 phosphorylation (Fig. 4I), especially in the case of the ΔUL13 mutant. Note that PRDX1 expression was downregulated in cells infected by wild-type and ΔUL13R rescued viruses but not in cells infected by the ΔUL13 mutant. These data

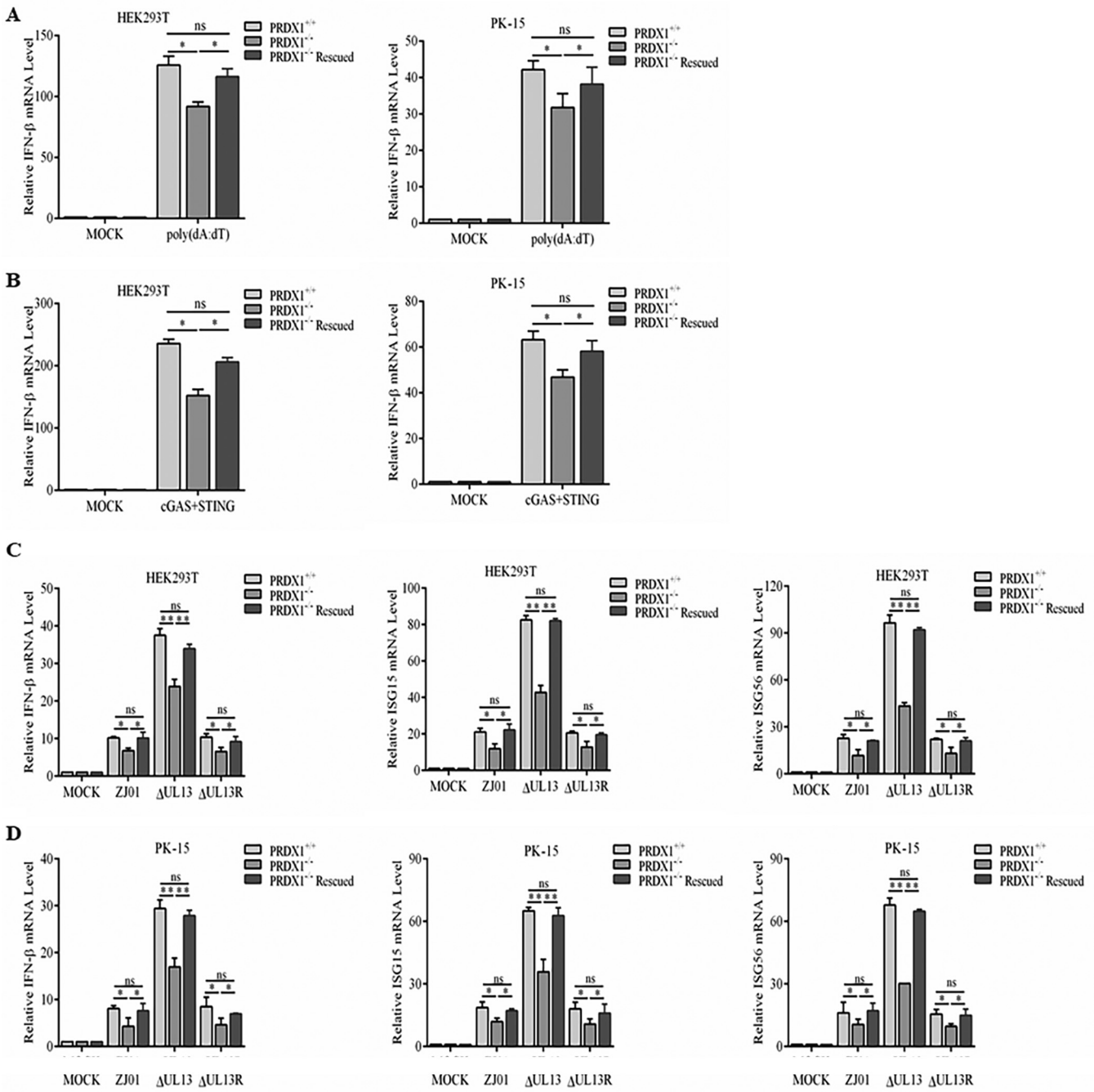

FIG 3 PRDX1 deficiency attenuates antiviral immunity. Effects of PRDX1 on antiviral gene expression during PRV infection were assessed. (A and B) PRDX1$^{+/+}$, PRDX1$^{-/-}$, and PRDX1$^{-/-}$ rescued HEK293T or PK-15 cells were mock transfected or transfected with poly(dA-dT) (1 μg/ml) or cGAS-Flag (100 ng) and STING-Flag (100 ng). After 24 h, total RNA was extracted from the cells and subjected to qRT-PCR analysis for quantitation of IFN-β and poly (dA-dT) (A) or cGAS plus STING (B). (C and D) PRDX1$^{+/+}$, PRDX1$^{-/-}$, and PRDX1$^{-/-}$ rescued HEK293T or PK-15 cells were mock infected or infected with ZJ01, ΔUL13, or ΔUL13R at an MOI of 0.1. Twelve hours after infection, total RNA was extracted from cells and subjected to qRT-PCR analysis for quantitation of IFN-β, ISG15, and ISG56 in HEK293T cells (C) and PK-15 cells (D). Cells were infected and processed as for panels A and B. Data were normalized using β-actin, and levels were calculated as described in Materials and Methods. Results are expressed as fold activation with standard deviations for triplicate samples. One-way analysis of variance (ANOVA) was used for multiple comparisons (Sidak's multiple-comparison test). ns, not significant ($P > 0.05$); *, $P < 0.05$. **, $P < 0.01$.

revealed that PRDX1 regulates IFN-β production through TBK1 and IKKε and that UL13 may counter cellular defenses by reducing PRDX1 levels.

UL13 specifically promotes PRDX1 degradation. To determine how UL13 affects PRDX1 expression, HEK293T and PK-15 cells were separately transfected with H-PRDX1-Myc (from *Homo sapiens*) or S-PRDX1-Myc (from *Sus scrofa*), together with increasing doses

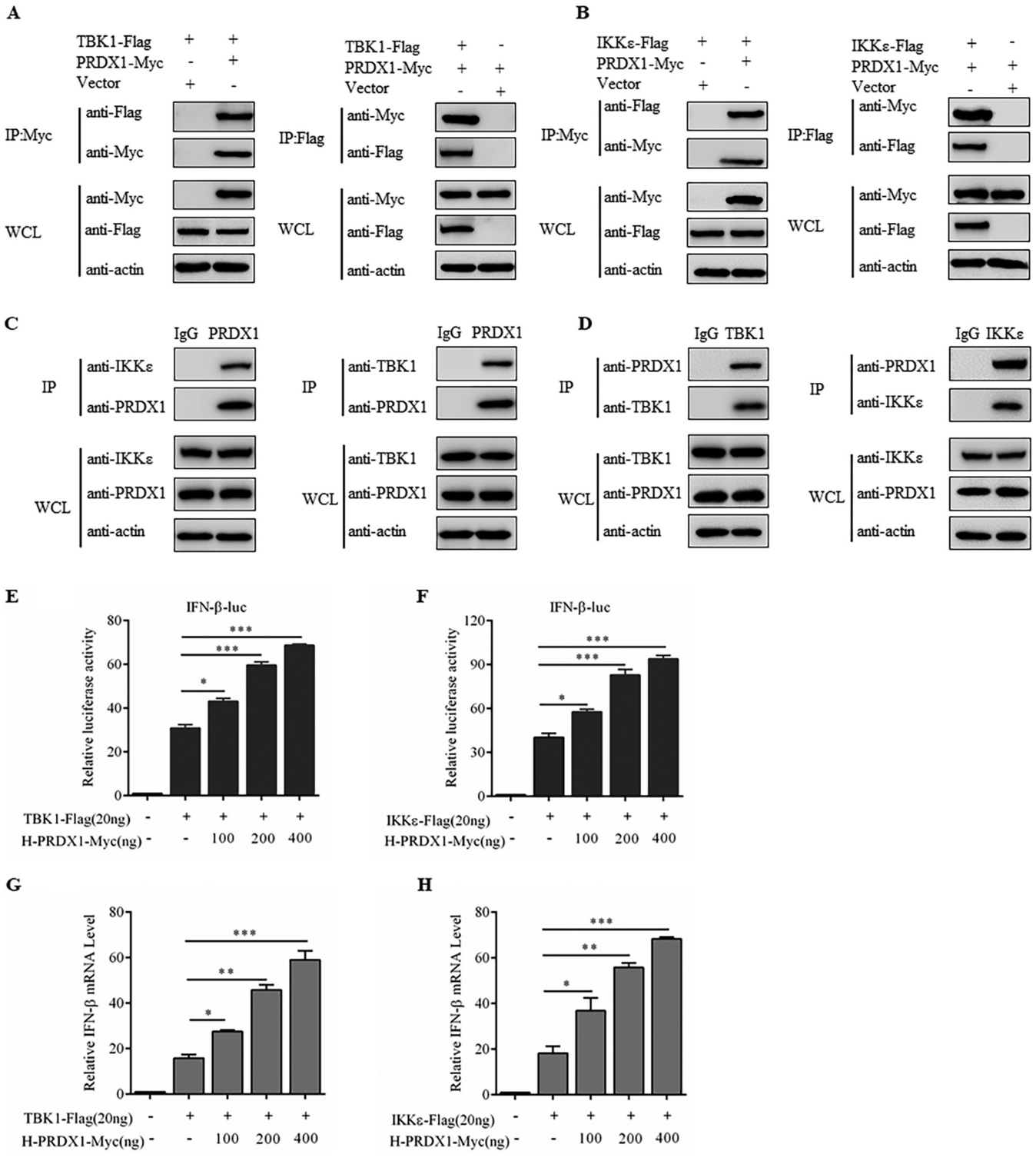

FIG 4 (Continued).

of UL13-Flag or green fluorescent protein (GFP)-Flag as controls. Western blot assays showed that PRDX1 expression decreased in response to increasing UL13 transfection, while the GFP control had no effect (Fig. 5A and B). The results suggest that UL13 specifically modulates degradation of the PRDX1 protein.

Since UL13 is a member of the CHPKs (6), we asked whether PRV UL13 has serine/

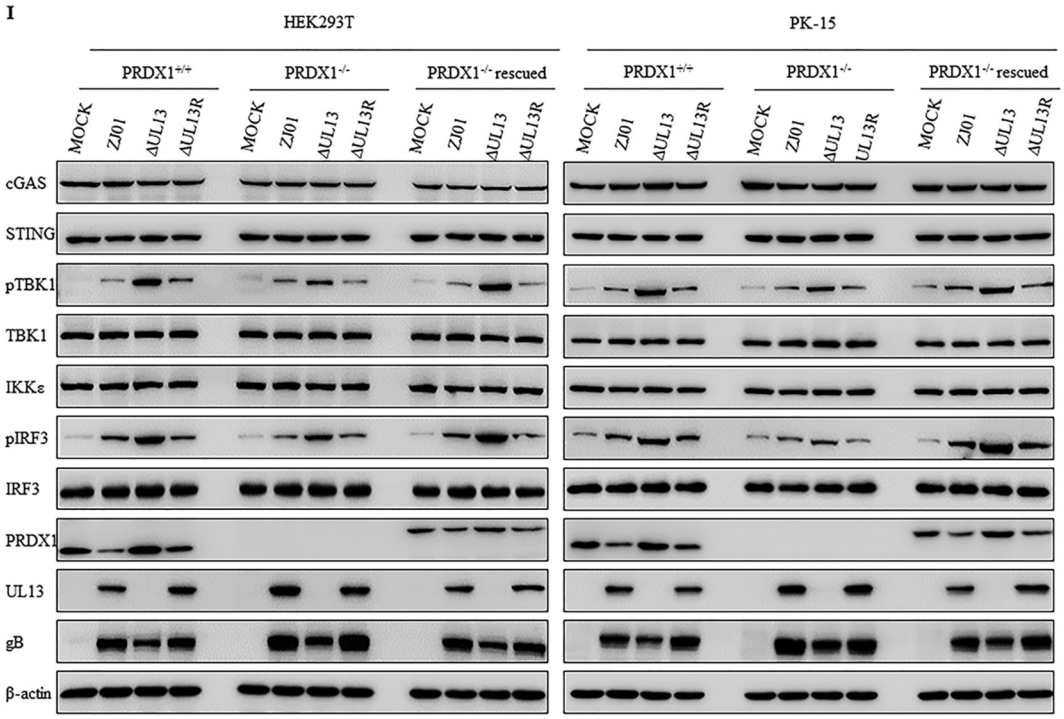

FIG 4 Identification of PRDX1 as a positive regulator of IFN-β signaling. (A and B) Co-IP and immunoblot analyses. HEK293T cells were transfected with PRDX1-Myc (3 μg) together with TBK1-Flag (3 μg) (A) or IKKε-Flag (3 μg) (B) for 30 h. Cell extracts were subjected to immunoprecipitation (IP) with the indicated antibodies, and precipitated proteins and whole-cell lysates (WCL) were probed using antibodies against Myc, Flag, or β-actin. (C and D) HEK293T cells (2×10^6 cells) were plated in 6-well dishes and incubated for 30 h. Cell lysates were subjected to immunoprecipitation assays using IgG (1 μg/ml) or anti-TBK1 (1 μg/ml), anti-IKKε (1 μg/ml), and anti-PRDX1 (1 μg/ml) antibodies. (E and F) Effects of PRDX1 on TBK1-induced (E) and IKKε-induced (F) IFN-β promoter activity. HEK293T cells were transfected with TBK1-Flag or IKKε (20 ng) and various amounts of PRDX1-Myc along with an IFN-β reporter. After 24 h, cells were harvested for luciferase assays. (G and H) Effects of PRDX1 on TBK1-induced (G) and IKKε-induced (H) IFN-β mRNA expression. HEK293T cells were transfected with TBK1-Flag or IKKε (20 ng) and various amounts of PRDX1-Myc. After 24 h, total RNA was extracted from cells and subjected to qRT-PCR analysis as described in Materials and Methods. (I) Effects of PRDX1 on the IFN pathway during PRV infection. HEK293T and PK15 cells were mock infected or infected with the indicated viruses (MOI of 0.1). Twelve hours after infection, cell lysates were prepared and subjected to Western blot analysis with antibodies against cGAS, STING, phosphorylated TBK1, TBK1, IKKε, phosphorylated IRF3, IRF3, PRDX1, UL13, gB, or β-actin. The results shown are representative of three independent experiments. Differences were assessed using one-way ANOVA. *, $P < 0.05$; **, $P < 0.01$; ***, $P < 0.001$.

threonine kinase activity and plays a role in the reduction of PRDX1 protein levels. Based on a comparison of UL13 amino acid sequences from PRV strains with homologous proteins from different alphaherpesviruses (HSV-1 and HSV-2), we constructed a PRV UL13 mutant with a mutation at K93 (UL13/K93A-Flag) and an HSV-1 UL13 mutant with a mutation at K176 (H-UL13/K176A-Flag). K93 is the conserved protein kinase site in PRV UL13 (Fig. 5C and D) and is functionally identical to K176 in HSV-1 UL13 (see Fig. S4). The PRV UL13/K93A mutant does not downregulate PRDX1 expression in either HEK293T or PK-15 cells, while wild-type UL13 retains this ability (Fig. 5C and D). To further explore the effect of PRV infection on endogenous PRDX1 degradation, HEK293T or PK-15 cells were infected with ZJ01, ΔUL13, or ΔUL13R, and PRDX1 expression was examined using Western blots. The results showed that ΔUL13 lost the ability to downregulate PRDX1 expression, compared with the wild-type virus and ΔUL13R (Fig. 5E to H). Together, these results suggest that UL13 requires its kinase activity to promote the degradation of PRDX1.

UL13 primes PRDX1 for proteolysis in the proteasome degradation pathway via K48-linked ubiquitination. The ubiquitin-proteasome system, the autolysosome pathway, and apoptosis are the three major intracellular protein degradation pathways (36–38). To determine which pathway is responsible for UL13-mediated PRDX1 degradation, the proteasome inhibitor MG132 (1 μM or 5 μM), the autophagy inhibitor 3-methyladenine (3-MA) (1 mM or 5 mM), and the apoptosis inhibitor Z-VAD-FMK (carbobenzoxy-valyl-alanyl-

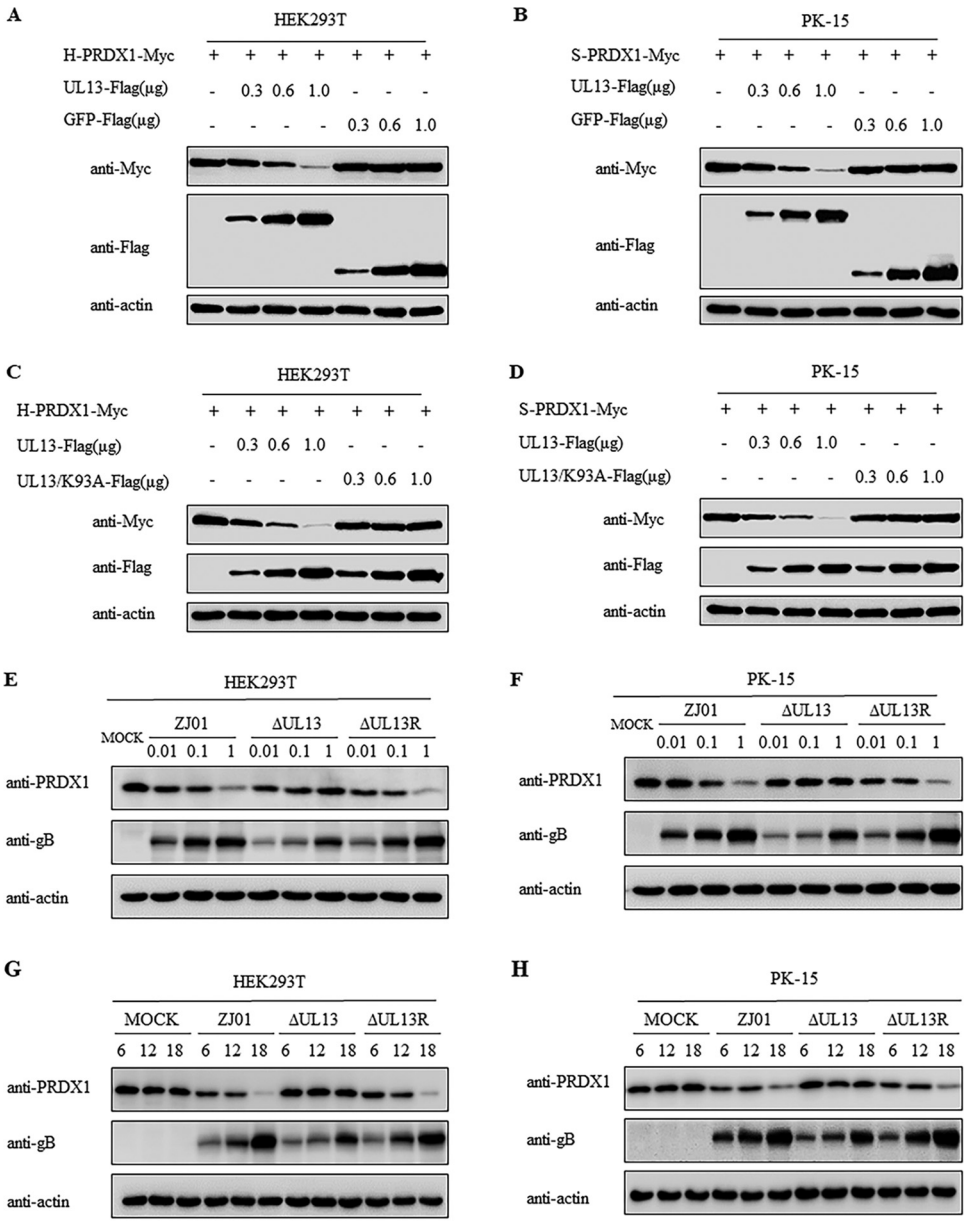

FIG 5 UL13 specifically promotes PRDX1 degradation. (A and B) HEK293T or PK-15 cells were separately transfected with H-PRDX1-Myc (A) or S-PRDX1-Myc (B) (500 ng) and increasing amounts of UL13-Flag or GFP-Flag. After 24 h, cell lysates were collected and subjected to Western blot analysis using antibodies against Myc, Flag, and β-actin. (C and D) HEK293T or PK-15 cells were transfected with H-PRDX1-Myc (C) or H-PRDX1-Myc (D) (500 ng) and increasing amounts of UL13-Flag or UL13/K93A-Flag. After 24 h, cell lysates were prepared and processed as described for panels A and B. Results shown are representative of three independent experiments. (E and F) HEK293T (E) or PK-15 (F) cells were mock infected or infected with ZJ01, ΔUL13, or ΔUL13R at an MOI of 0.01, 0.1, or 1. After 12 h, cells were subjected to Western blot analysis using the indicated antibody. (G and H) HEK293T (G) or PK-15 (H) cells were mock infected or infected with ZJ01, ΔUL13, or ΔUL13R at an MOI of 0.1. Cells were harvested at 6, 12, and 18 h after infection for Western blot analysis with the indicated antibodies.

aspartyl-[*O*-methyl]-fluoromethylketone) (1 μM or 5 μM) were added to cells cotransfected with the PRDX1-Myc and UL13-Flag expression constructs. As shown in Fig. 6A, MG132 treatment almost completely restored PRDX1 expression levels. To examine this more closely, HEK293T cells were infected with PRV ZJ01 and treated with MG132. Western blot analysis showed that PRDX1 expression was largely restored by MG132 treatment (Fig. 6B). The results indicate that UL13 routes PRDX1 into proteasomes for degradation.

Because ubiquitination is typically involved in the proteasome-dependent degradation

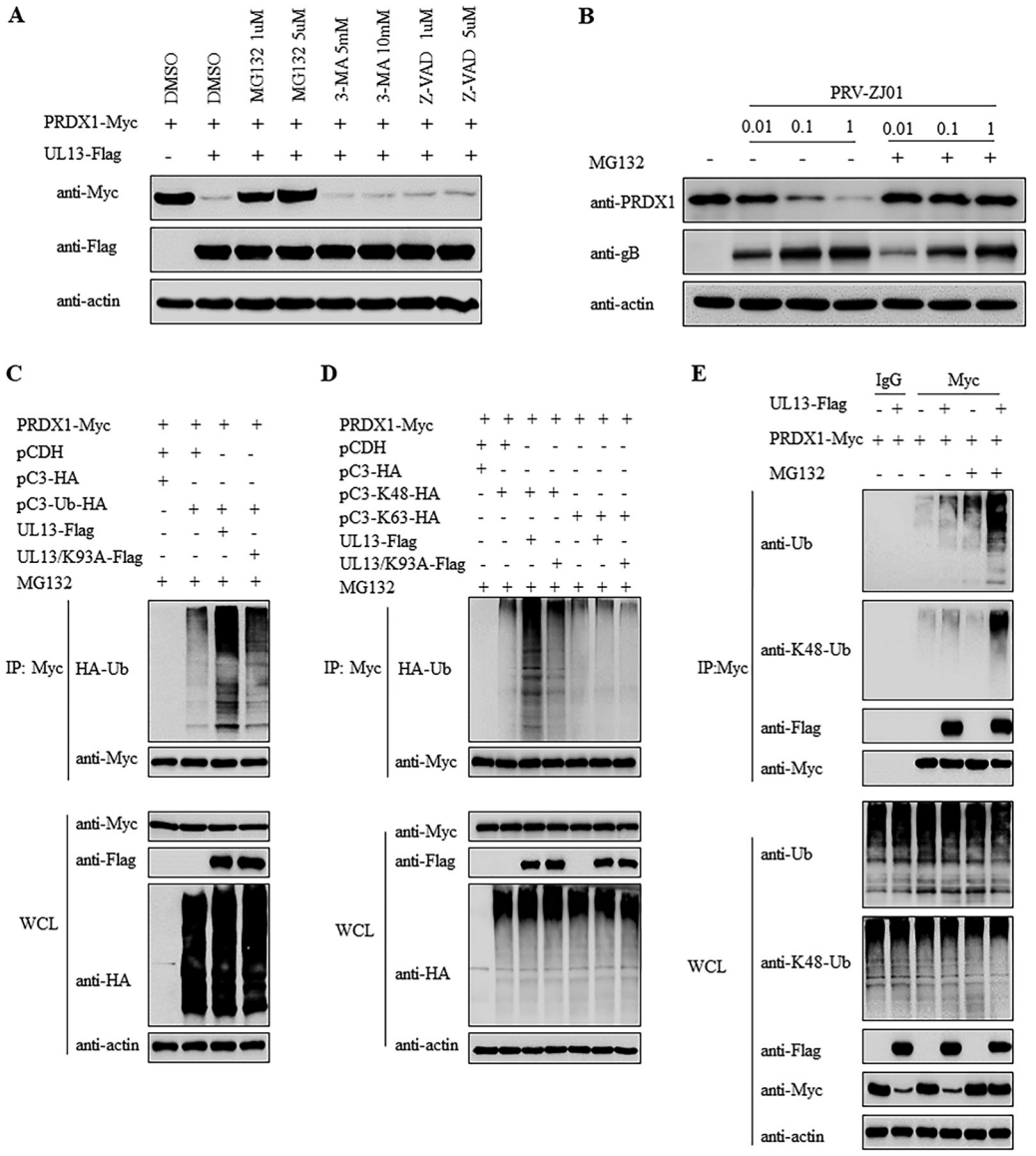

FIG 6 UL13 tags PRDX1 for degradation in the proteasome pathway via K48-linked ubiquitination. (A) Effect of MG132, 3-MA, or Z-VAD-FMK on PRDX1 degradation. HEK293T cells were transfected with UL13-Flag (1,000 ng) and PRDX1-Myc (500 ng). After 20 h, cells were treated with dimethyl sulfoxide and different concentrations of MG132, 3-MA, or Z-VAD-FMK for 8 h and then were harvested for Western blot analysis using antibodies against Myc, Flag, and β-actin. (B) Effect of MG132 on PRDX1 degradation during PRV infection. HEK293T cells were mock infected or infected with ZJ01 at an MOI of 0.01, 0.1, or 1. After 6 h, cells were treated with or without MG132 (5 μM) for 8 h and then harvested for Western blot analysis using antibodies against PRDX1, gB, and β-actin. (C) Effects of UL13 on PRDX1 ubiquitination. HEK293T cells were transfected with various combinations of plasmids encoding Myc-PRDX1 (3 μg), UL13-Flag (3 μg), UL13/K93A-Flag (3 μg), and HA-ubiquitin (3 μg). After 20 h, cells were treated with MG132 (5 μM) for 8 h, harvested, and analyzed by immunoprecipitation (IP) using the Myc tag. Whole-cell lysates (WCL) and immunoprecipitates were analyzed by Western blotting using antibodies against HA, Myc, Flag, and β-actin. (D) UL13 promotes K48-linked ubiquitination of PRDX1. HEK293T cells were transfected with various combinations of plasmids encoding Myc-PRDX1 (3 μg), UL13-Flag (3 μg), UL13/K93A-Flag (3 μg), and HA-ubiquitin (K48) (3 μg) or HA-ubiquitin (K63) (3 μg). Methods were identical to those described for panel B. (E) Effects of UL13 on endogenous ubiquitination of PRDX1. HEK293T cells were transfected with PRDX1-Myc (3 μg) and UL13-Flag (3 μg) for 20 h, followed by treatment with MG132 (5 μM) for 8 h. Cell extracts were subjected to immunoprecipitation with anti-Myc monoclonal antibody, followed by Western blot analysis using antibodies against endogenous ubiquitin and K48 chains. Results are representative of three independent experiments.

pathway (39), we evaluated the effect of UL13 on PRDX1 ubiquitination. As shown in Fig. 6C, PRDX1 ubiquitination increased significantly in the presence of UL13 and MG-132, but ubiquitination was not affected when UL13/K93A was substituted for UL13. We then determined that UL13 markedly increased K48-linked ubiquitination of PRDX1 but not K63-linked ubiquitination (Fig. 6D). Overexpression of UL13 significantly enhanced

endogenous ubiquitination and K48-linked ubiquitination (Fig. 6E). These data reveal that UL13 promotes PRDX1 degradation in the proteasome-dependent pathway via K48-linked polyubiquitination.

UL13 serine/threonine kinase activity plays a critical role in antiviral immunity and virus replication. To evaluate the relationships between the serine/threonine kinase activity of UL13, the PRDX1-mediated IFN response, and virus replication, a recombinant PRV containing a mutation (UL13/K93A) and its rescued counterpart (UL13/K93AR) were constructed. Plaques formed by UL13/K93A were smaller than those formed by UL13/K93AR and wild-type ZJ01 in PK-15 cells (see Fig. S2). The mutant and rescued viruses were used to infect PRDX1$^{+/+}$, PRDX1$^{-/-}$, and PRDX1$^{-/-}$ rescued HEK293T and PK-15 cells. Following infection, cytokine and ISG expression levels were measured using qRT-PCR and enzyme-linked immunosorbent assay (ELISA). The results showed that ΔUL13 and UL13/K93A significantly induced expression of IFN-β, ISG15, and ISG56 in PRDX1$^{+/+}$ and PRDX1$^{-/-}$ rescued HEK293T and PK-15 cells, compared to UL13/K93AR and wild-type ZJ01 (Fig. 7A to D). The results suggest that viral UL13 and its serine/threonine kinase activity site (K93) act to inhibit antiviral immunity. In addition, cytokine and ISG expression levels in PRDX1$^{-/-}$ HEK293T and PK-15 cells were greatly diminished, compared to those in wild-type and PRDX1$^{-/-}$ rescued cells, suggesting that PRDX1 plays a critical role in PRV infection. Replication of ZJ01, ΔUL13, UL13/K93A, and UL13/K93AR in PRDX1$^{-/-}$ HEK293T and PK-15 cells was increased, compared to replication in wild-type and PRDX1$^{-/-}$ rescued cells. Finally, growth of ΔUL13 and UL13/K93A was largely restored in PRDX1$^{-/-}$ HEK293T and PK-15 cells (Fig. 7E and F). Together, the data indicate that UL13 serine/threonine kinase activity plays an important role in PRV replication.

DISCUSSION

PRV, a member of the alphaherpesvirus subfamily, can conduct lytic replication or persist as a latent infection in the cell (1, 40). In the lytic replication cycle, the virus orchestrates gene expression, DNA replication, assembly, and egress. During this process, PRV provokes several antiviral innate immune responses that operate coordinately. Our previous study demonstrated that UL13 protein inhibits the IFN pathway by targeting IRF3. In the present study, PRDX1 was shown to interact with PRV UL13. It also interacts with TBK1/IKKε and promotes their function as mediators of IFN activation and negatively regulates PRV propagation. Finally, PRV UL13 ubiquitinates PRDX1 (via K48), shunting PRDX1 into proteasomes for eventual degradation.

PRDXs are a family of antioxidant enzymes that regulate cytokine-induced peroxide levels, affecting multiple signal transduction pathways (41–43). The structure of the peroxidatic active site is highly conserved in PRDX1 through PRDX6. PRDX1, also known as MSP23, is an abundant protein with an approximate molecular mass of 23 kDa (44). PRDX1 has been identified as an induced macrophage redox protein with multiple functions. Additionally, extracellular PRDX1 plays a critical role in the regulation of inflammation and cancer development. PRDX1 is associated with the occurrence, growth, and metastasis of a variety of cancers, such as breast cancer and esophageal cancer (45, 46). PRDX1 knockout fibroblasts display decreased proliferation and increased susceptibility to oxidative DNA damage (41). PRDX1 knockout mice exhibit abnormalities in the number and phenotype of natural killer (NK) cells and develop a high frequency of intestinal malignancies, sarcomas, and lymphomas, suggesting that PRDX1 plays a role in cancer progression (47). PRDX1 has also been found to negatively regulate NF-κB signaling activation and autophagy functions by inhibiting TRAF6 ubiquitin ligase activity (48). However, little is known about the role of PRDX1 in regulating innate immunity. Our data demonstrate that PRDX1 functions in the type I IFN pathway by interacting with TBK1 and IKKε.

TBK1 and IKKε are members of the IKK family and are best known for their indispensable roles in the type I IFN signaling pathway. The pathway is activated by diverse host pattern recognition receptors (PRRs) in response to a variety of DNA or RNA viruses, including the alphaherpesviruses (23, 49, 50). Both TBK1 and IKKε are modified by activation loop phosphorylation (S172) to induce target phosphorylation (50). Most critically, the activity of the TBK1/IKKε complex is regulated by various molecules

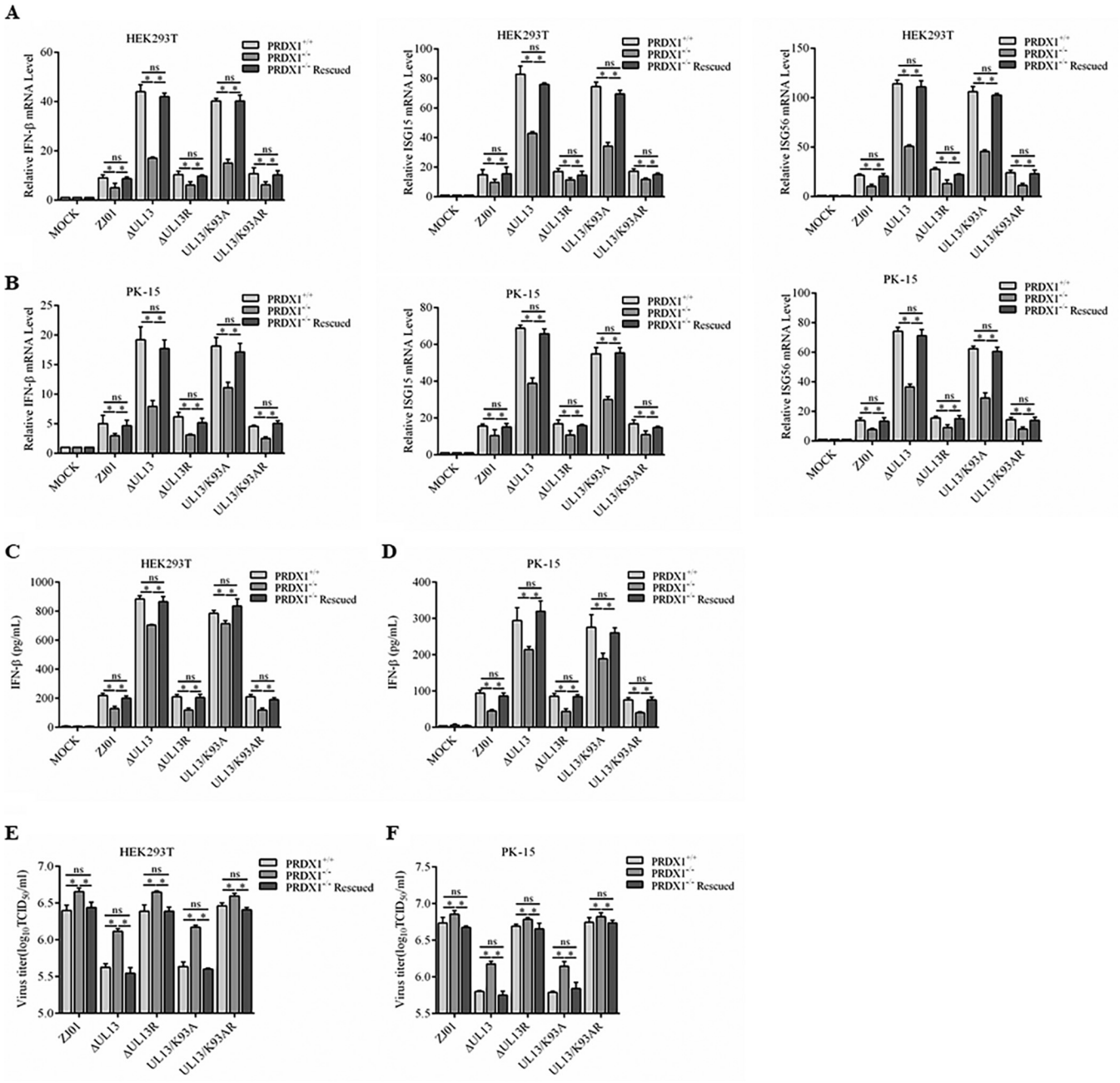

FIG 7 The serine/threonine kinase activity of UL13 affects antiviral immunity and virus replication. (A to D) PRDX1$^{+/+}$, PRDX1$^{-/-}$, and PRDX1$^{-/-}$ rescued HEK293T (A and C) or PK-15 (B and D) cells were either mock infected or infected with ΔUL13, the UL13/K93A mutant, or the rescued virus UL13/K93AR (MOI of 0.1). After 12 h, total RNA was extracted from the cells and subjected to qRT-PCR to quantitate IFN-β, ISG15, and ISG56 expression (A and B). The data were normalized using β-actin. IFN-β levels in the cell supernatants were detected using a pig or human IFN-β ELISA kit, according to the manufacturer's instructions (C and D). (E and F) Viral replication in PRDX1$^{+/+}$, PRDX1$^{-/-}$, and PRDX1$^{-/-}$ rescued HEK293T (E) or PK-15 (F) cells. Cells were infected with ΔUL13, the UL13/K93A mutant, or UL13/K93AR at an MOI of 0.01. After 24 h, cells were harvested and the total virus yields were determined on the designated cells. Virus yields are shown as $TCID_{50}$ per milliliter. Results are representative of three independent experiments, and differences were assessed by one-way ANOVA. ns, not significant ($P > 0.05$); *, $P < 0.05$.

through multiple diverse posttranslational modifications, such as ubiquitination, deubiquitination, and phosphorylation (24, 25, 29, 30). In this study, our results showed that PRDX1 positively regulates TBK1/IKKε-mediated IFN activation by interacting with these factors. This is the first glimpse into the mechanism by which PRDX1 affects the innate immune pathway, and it is supported by our demonstration that a PRDX1 knockout led to a decrease of TBK1 and IRF3 phosphorylation after PRV virus infection. However, the detailed mechanism by which PRDX1 regulates the kinase activity of

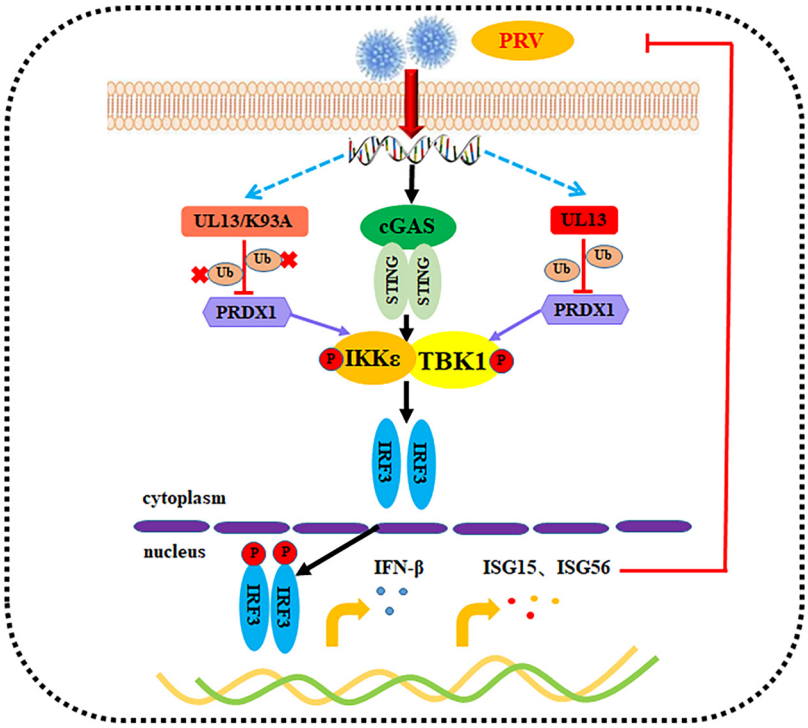

FIG 8 Model representing PRDX1 function in IFN-β signaling and its inhibition by PRV UL13. After PRV infection, PRDX1 accumulates and stimulates TBK1/IKKε-mediated IFN-β signaling, which depresses PRV proliferation. However, viral kinase protein UL13 promotes the degradation of PRDX1 and blocks its ability to stimulate IFN-β signaling.

TBK1/IKKε is still unclear. It is possible that PRDX1 acts directly on TBK1 via ubiquitination and deubiquitination to enhance kinase activity or stability, but this hypothesis requires further investigation.

To counteract host defenses, PRV-encoded UL13 promotes K48-linked ubiquitination and degradation of PRDX1, preventing PRDX1 from stimulating the immune response. UL13 and its serine/threonine kinase activity site (K93) also function to inhibit antiviral immunity. UL13 proteins are serine/threonine protein kinases encoded by alphaherpesviruses and are some of the many CHPKs found throughout the *Herpesviridae* family (6). UL13 regulates the expression of viral proteins, including ICP0, UL26, UL38, UL41, UL49, and Us11 (7, 10). However, studies of UL13 mutations and their effects on viral replication have yielded mixed results. Numerous reports show that HSV-1 UL13 protein kinase activity is critical for viral replication, but the results are cell type dependent. For example, an HSV-1 UL13 K176M mutation (which abolishes kinase activity) reduced replication by 10-fold, compared to wild-type virus (51). Similar results were obtained with HSV-2, in which a K176M mutation reduced replication to levels similar to those observed with the UL13-null virus in U2OS cells, but the reduction was not observed in Vero cells (IFN-deficient cell lines) (12). Previous work demonstrated that UL13 kinase activity promotes the evasion of HSV-1 in the central nervous system in mice, suggesting that UL13-mediated immune evasion is critical for viral replication and pathogenicity in the central nervous system (52). In contrast, studies involving UL13 in alphaherpesviruses have yielded inconsistent data. In some cases, the UL13 kinase appears to be dispensable for viral replication (8, 53). In PRV, a D194A mutation in UL13 attenuates transport of capsids to the distal axon, independent of replication (11). In our study, we found that UL13 and its serine/threonine protein kinases (Lys93) are important in viral replication, because they function to neutralize defenses imposed by the innate immune response.

In summary, we have found that PRDX1 negatively regulates PRV propagation by binding to TBK1 and IKKε and promoting type I IFN activation (Fig. 8). However, the PRV-encoded kinase UL13 functions as a countermeasure by binding and promoting

TABLE 1 Primers used in this study

Primer	Sequence (5′→3′)	Usage
Myc-H-PRDX1-F	CCAAGCTTATGTCTTCAGGAAATGCTAA	Amplification of human PRDX1
Myc-H-PRDX1-R	CGGAATTCTCACTTCTGCTTGGAGAAAT	
Myc-S-PRDX1-F	CCAAGCTTATGTCTTCAGGAAATGCCAA	Amplification of *Sus scrofa* PRDX1
Myc-S-PRDX1-R	CGGAATTCTCACTTCTGTTTAGAGAAAT	
UL13/K93A-F	TACGGCTCGGTGGCCGTGGCCACGCTCCGCGCCGGCTTC	Amplification of UL13 K93A
UL13/K93A-R	GAAGCCGGCGCGGAGCGTGGCCACGGCCACCGAGCCGTA	

PRDX1 K48-linked ubiquitination and degradation. Our results provide new insights into the interactions between PRV and the host immune response.

MATERIALS AND METHODS

Cells, viruses, antibodies, and reagents. HEK293T and PK-15 cells were obtained from the American Type Culture Collection (ATCC). PRV strain ZJ01 (GenBank accession number KM061380.1) was isolated in Zhejiang Province by our laboratory (54). MG132 (catalog number S2619), 3-MA (catalog number S2767), and Z-VAD-FMK (catalog number S7023) were purchased from Selleck Chemicals (USA). The following antibodies were used for Co-IP and Western blot experiments: anti-Flag (1:5,000; catalog number ab125243), anti-Myc (1:5,000; catalog number ab32), anti-PRDX1 (1:1,000; catalog number ab16745) (for Co-IP), and anti-GFP (1:2,500; catalog number ab290) from Abcam (UK), anti-hemagglutinin (HA) (1:5,000; catalog number 3724), anti-β-actin (1:5,000; catalog number 3700), polyclonal anti-IRF3 (1:1,000; catalog number 4302), anti-IRF3 phosphorylated at S396 (1:1,000; catalog number 83611), anti-cGAS (1:1,000; catalog number 31659), anti-STING (1:1,000; catalog number 13647), anti-TBK1 phosphorylated at S172 (1:1,000; catalog number 5483), anti-TBK1 (1:1,000; catalog number 3504), and anti-IKKε (1:2,000; catalog number 3416) from Cell Signaling Technology (USA), and anti-PRDX1 (1:5,000; catalog number 66820-1-Ig) from Proteintech Group (China). Anti-UL13 and anti-glycoprotein B (gB) antibodies were generated in our laboratory and are described elsewhere (14). Lipofectamine 3000 (L3000015) was used for plasmid transfection and was obtained from Thermo Fisher Scientific (USA).

Plasmid construction. The PRDX1 gene (GenBank accession numbers NC_000001.11 and NC_010448.4) was amplified from HEK293T and PK-15 cells and then cloned using the HindIII and EcoRI sites of pCDNA3.1, a vector that contains a C-terminal Myc tag. The clones were designated H-PRDX1-Myc and S-PRDX1-Myc, respectively. The UL13-Flag, GFP-Flag, pC3-Ub-HA, pC3-K48-HA, and pC3-K63-HA expression plasmids are described elsewhere (14). PRV UL13 point mutation K93A (UL13/K93A-Flag) and HSV-1 (F strain) UL13 point mutation K176A (H-UL13/K176A-Flag) were introduced using QuikChange II site-directed mutagenesis (catalog number 200524; Agilent) and cloned into the pCDH vector. This plasmid expresses the GFP cassette driven by a cytomegalovirus (CMV) promoter to replace the PRV UL13 open reading frame region cloned into the pUC-19 vector and was named pUC-CMV-GFP. The plasmids cGAS-Flag, STING-Flag, TBK1-Flag, IKKε-Flag, pIFN-β-Luc, and pTK-Luc are described elsewhere (14). All PCR primers are listed in Table 1.

ESI-MS. HEK293T cells were transfected with a UL13-Flag (3 μg) construct or with empty vector (pCDH). The cells were harvested 48 h after transfection and then lysed on ice in RIPA lysis buffer (50 mM Tris-HCl [pH 8], 1% Nonidet P-40, 150 mM NaCl, 0.5% sodium deoxycholate, 0.1% SDS) supplemented with 1 mM phenylmethylsulfonyl fluoride (PMSF). After centrifugation at 10,000 $\times$ *g* for 10 min, the supernatants were incubated with 1 μg mouse antibody and 30 μl protein A/G-agarose beads at 4°C for 3 h. The supernatants were collected, immunoprecipitated with 1 μg anti-Flag monoclonal antibody at 4°C for 12 h, and then mixed with 30 μl of protein A/G-agarose beads at 4°C for 4 h. The immunoprecipitated protein complexes were centrifuged for 5 min at 5,000 rpm at 4°C, and the supernatant containing total proteins was collected and subjected to nano-liquid chromatography-tandem mass spectrometry (nano-LC-MS/MS) analysis by Shanghai Applied Protein Technology (Shanghai, China). LC-MS/MS analysis was performed for 120 min on a Q Exactive mass spectrometer (Thermo Fisher Scientific) coupled to an EASY-nLC injector (Proxeon Biosystems; Thermo Fisher Scientific). The mass spectrometer was operated in positive-ion mode. MS data were acquired using a data-dependent top 10 method dynamically choosing the most abundant precursor ions from the survey scan (*m/z* 300 to 1,800) for higher energy collisional dissociation fragmentation. MS/MS spectra were searched, using the MASCOT engine v2.2 (Matrix Science, London, UK) embedded in Proteome Discoverer v1.4 (Thermo Fisher Scientific), against the UniProt human database (133,549 sequences, download on 3 March 2013) and the decoy database. For protein identification, the following options were used: peptide mass tolerance = 20 ppm, MS/MS tolerance = 0.1 Da, enzyme = trypsin, missed cleavage = 2, fixed modification = carbamidomethyl (C), variable modification = oxidation (M), and false discovery rate (FDR) = $\leq$0.01.

Transfection and dual luciferase reporter assays. HEK293T cells (2×10^5 cells) were cultured in 12-well plates and then transfected with the expression plasmids along with pIFN-β-Luc (100 ng) or the empty vector (negative control) pGL3 (100 ng) and the *Renilla* luciferase construct (pRL-TK) (20 ng), which served as an internal control. Twenty-four hours after transfection, cells were lysed and luciferase activity was measured using a dual luciferase reporter assay system (Promega), following the manufacturer's instructions. Relative luciferase activity was normalized to the control value.

qRT-PCR. For qRT-PCR, total RNA was isolated from HEK293T and PK-15 cells using the total RNA kit (Omega) and reverse transcribed into cDNA according to the manufacturer's instructions. qRT-PCR was

performed using SYBR green real-time PCR Master Mix and an ABI QuantStudio 7 real-time PCR system (Applied Biosystems). The specific primer sequences for the targeting genes were described previously (14).

ELISA. HEK293T cells and PK-15 cells were infected with PRV at a multiplicity of infection (MOI) of 0.1 and incubated for 12 h. IFN-β levels in cell supernatants were detected using a human IFN-β ELISA kit (Elabscience, Wuhan, China) or a pig IFN-β ELISA kit (Mlbio, Shanghai, China), according to the manufacturer's instructions (55).

Western blot analysis. Cell lysates and immunoprecipitates were subjected to 10% SDS-PAGE and then transferred to polyvinylidene difluoride (PVDF) membranes. The membranes were blocked for 2 h at room temperature in Tris-buffered saline (TBS) containing 10% nonfat dry milk and 0.05% Tween 20 and were incubated at room temperature for 2 h with the indicated antibodies. Membranes were washed with 1× TBS containing Tween 20, incubated with horseradish peroxidase (HRP)-labeled goat anti-rabbit IgG or anti-mouse IgG antibody at room temperature for 1 h, and treated with enhanced chemiluminescence (ECL) reagent (Thermo Fisher Scientific).

Co-IP. HEK 293T cells were transfected with expression plasmids and incubated for 30 h. The cells were washed in prechilled phosphate-buffered saline (PBS) and lysed with cell lysis buffer as described elsewhere (56). For Co-IP assays, cell lysates were centrifuged at 10,000 × *g* for 5 min. The supernatants were incubated with 1 μg of homograft mouse or rabbit antibody and 30 μl of protein A/G-agarose beads (Beyotime, China) at 4°C for 3 h. Supernatants were collected, incubated with 1 μg of the designated antibody at 4°C for 12 h, and then each lysate was combined with 30 μl of protein A/G-agarose and incubated at 4°C for 3 h. Lysates were centrifuged at 2,500 × *g* for 5 min to collect the beads and were washed five times with prechilled PBS. Finally, the immunoprecipitates were subjected to Western blot analysis.

Generation of PRV containing UL13 deletions or site-specific mutations. To generate ZJ01 virus containing UL13 deletions, PK-15 cells were transfected with ZJ01 genome (500 ng), the CRISPR/Cas9 system plasmid PX335-sgRNA containing two targeting single guide RNAs (sgRNAs) for ZJ01 UL13 (designated pX335-UL13-1 and pX335-UL13-2), and the GFP cassette expression plasmid (pUC-CMV-GFP) (500 ng). All primers are listed in Table S1 in the supplemental material. After PRV-mediated cytopathogenic effects were evident in the transfected cells, viruses were harvested and stored at −80°C. The recombinant UL13 deletion (GFP-substituted) PRV was purified by plaque assay, and the mutant lacking UL13 (ZJ01-ΔUL13-GFP) was identified using PCR.

To generate site-specific mutations in the ZJ01 virus, PK-15 cells were transfected with the ZJ01-ΔUL13-GFP genome (500 ng), the CRISPR/Cas9 system plasmid (500 ng) PX335-sgRNA containing two targeting sgRNAs for GFP (designated pX335-GFP-1 and pX335-GFP-2), and UL13 site-directed mutagenesis pUC-UL13/K93A. Primers are shown in Table 1. Plaque purification was performed to obtain a virus containing a UL13 site-specific mutation (ZJ01-UL13/K93A). ZJ01-ΔUL13-GFP and ZJ01-UL13/K93A-revertent virus was obtained by the same method. Constructs were sequenced using the primers listed in Table S1.

Viral plaque assays. Viral plaque assays were performed as described previously (14). Virus infectivity was quantified by infecting a PK-15 cell monolayer overlaid with 1% low-melting-point agarose and 1× Dulbecco's modified Eagle's medium (DMEM) (containing 2% heat-inactivated fetal bovine serum). After 3 days, cells were stained with 1% crystal violet in methanol for 12 h at room temperature, and plaques were counted.

Generation of cells with gene disruptions. To generate PRDX1$^{-/-}$ HEK293T knockout cells, pX459-sgRNA-puro plasmids targeting the human PRDX1 gene were transfected into 2×10^5 HEK293T cells. Twenty-four hours later, positive (puromycin-resistant) cells were transferred as single clones to a 96-well plate. Candidate clones were screened by PCR and sequencing of the PCR products to confirm the gene knockout. As a second test, clones were also subjected to Western blot analysis using PRDX1 antibodies. To generate PRDX1$^{-/-}$ PK-15 knockout cells, the lentiCRISPRv2 system was used. PK-15 cells (2×10^5 cells) were infected with a lentivirus construct that expressed a sgRNA-puromycin plasmid targeting the *Sus scrofa* PRDX1 gene. Two days later, positive (puromycin-resistant) cells were transferred to a 96-well plate. Cell clones with the desired gene knockout were identified by Western blot analysis using the appropriate antibodies The HEK293T and PK-15 PRDX1 sgRNA targeting site was designed using Benchling (https://www.benchling.com/crispr). The sgRNA sequence and PCR sequencing primers are listed in Table S1 in the supplemental material.

SUPPLEMENTAL MATERIAL

Supplemental material is available online only.

SUPPLEMENTAL FILE 1, PDF file, 1 MB.

ACKNOWLEDGMENTS

This work was supported by the National Key Program of Research and Development of China (grant 2016YFD0500105), the China Agricultural Research System Foundation (grant CARS-36), and a grant from Jiangsu Province (grant PAPD).

REFERENCES

1. Tanaka S, Imamura T, Sakaguchi M, Mannen K. 1998. Acetylcholine reactivates latent pseudorabies virus in mice. J Virol Methods 70:103–106. https://doi.org/10.1016/s0166-0934(97)00174-2.

2. Klupp BG, Hengartner CJ, Mettenleiter TC, Enquist LW. 2004. Complete, annotated sequence of the pseudorabies virus genome. J Virol 78:424–440. https://doi.org/10.1128/jvi.78.1.424-440.2004.

3. Cheung AK. 1996. Latency characteristics of an EPO and LLT mutant of pseudorabies virus. J Vet Diagn Invest 8:112–115. https://doi.org/10.1177/104063879600800119.
4. Pomeranz LE, Reynolds AE, Hengartner CJ. 2005. Molecular biology of pseudorabies virus: impact on neurovirology and veterinary medicine. Microbiol Mol Biol Rev 69:462–500. https://doi.org/10.1128/MMBR.69.3.462-500.2005.
5. Jacob T, Van den Broeke C, Favoreel HW. 2011. Viral serine/threonine protein kinases. J Virol 85:1158–1173. https://doi.org/10.1128/JVI.01369-10.
6. Kawaguchi Y, Kato K. 2003. Protein kinases conserved in herpesviruses potentially share a function mimicking the cellular protein kinase cdc2. Rev Med Virol 13:331–340. https://doi.org/10.1002/rmv.402.
7. Eaton HE, Saffran HA, Wu FW, Quach K, Smiley JR. 2014. Herpes simplex virus protein kinases US3 and UL13 modulate VP11/12 phosphorylation, virion packaging, and phosphatidylinositol 3-kinase/Akt signaling activity. J Virol 88:7379–7388. https://doi.org/10.1128/JVI.00712-14.
8. Purves FC, Roizman B. 1992. The UL13 gene of herpes simplex virus 1 encodes the functions for posttranslational processing associated with phosphorylation of the regulatory protein alpha 22. Proc Natl Acad Sci U S A 89:7310–7314. https://doi.org/10.1073/pnas.89.16.7310.
9. Ogle WO, Ng TI, Carter KL, Roizman B. 1997. The UL13 protein kinase and the infected cell type are determinants of posttranslational modification of ICP0. Virology 235:406–413. https://doi.org/10.1006/viro.1997.8710.
10. Asai R, Ohno T, Kato A, Kawaguchi Y. 2007. Identification of proteins directly phosphorylated by UL13 protein kinase from herpes simplex virus 1. Microbes Infect 9:1434–1438. https://doi.org/10.1016/j.micinf.2007.07.008.
11. Coller KE, Smith GA. 2008. Two viral kinases are required for sustained long distance axon transport of a neuroinvasive herpesvirus. Traffic 9:1458–1470. https://doi.org/10.1111/j.1600-0854.2008.00782.x.
12. Koyanagi N, Kato A, Takeshima K, Maruzuru Y, Kozuka-Hata H, Oyama M, Arii J, Kawaguchi Y. 2018. Regulation of herpes simplex virus 2 protein kinase UL13 by phosphorylation and its role in viral pathogenesis. J Virol 92:e00807-18. https://doi.org/10.1128/JVI.00807-18.
13. Bo Z, Miao Y, Xi R, Zhong Q, Bao C, Chen H, Sun L, Qian Y, Jung YS, Dai J. 2020. PRV UL13 inhibits cGAS-STING-mediated IFN-β production by phosphorylating IRF3. Vet Res 51:118. https://doi.org/10.1186/s13567-020-00843-4.
14. Lv L, Cao M, Bai J, Jin L, Wang X, Gao Y, Liu X, Jiang P. 2020. PRV-encoded UL13 protein kinase acts as an antagonist of innate immunity by targeting IRF3-signaling pathways. Vet Microbiol 250:108860. https://doi.org/10.1016/j.vetmic.2020.108860.
15. Akira S, Uematsu S, Takeuchi O. 2006. Pathogen recognition and innate immunity. Cell 124:783–801. https://doi.org/10.1016/j.cell.2006.02.015.
16. Takeuchi O, Akira S. 2010. Pattern recognition receptors and inflammation. Cell 140:805–820. https://doi.org/10.1016/j.cell.2010.01.022.
17. Sun L, Wu J, Du F, Chen X, Chen ZJ. 2013. Cyclic GMP-AMP synthase is a cytosolic DNA sensor that activates the type I interferon pathway. Science 339:786–791. https://doi.org/10.1126/science.1232458.
18. Unterholzner L, Keating SE, Baran M, Horan KA, Jensen SB, Sharma S, Sirois CM, Jin T, Latz E, Xiao TS, Fitzgerald KA, Paludan SR, Bowie AG. 2010. IFI16 is an innate immune sensor for intracellular DNA. Nat Immunol 11:997–1004. https://doi.org/10.1038/ni.1932.
19. Zhang Z, Yuan B, Bao M, Lu N, Kim T, Liu YJ. 2011. The helicase DDX41 senses intracellular DNA mediated by the adaptor STING in dendritic cells. Nat Immunol 12:959–965. https://doi.org/10.1038/ni.2091.
20. Almine JF, O'Hare CA, Dunphy G, Haga IR, Naik RJ, Atrih A, Connolly DJ, Taylor J, Kelsall IR, Bowie AG, Beard PM, Unterholzner L. 2017. IFI16 and cGAS cooperate in the activation of STING during DNA sensing in human keratinocytes. Nat Commun 8:14392. https://doi.org/10.1038/ncomms14392.
21. Hopfner K, Hornung V. 2020. Molecular mechanisms and cellular functions of cGAS-STING signalling. Nat Rev Mol Cell Biol 21:501–521. https://doi.org/10.1038/s41580-020-0244-x.
22. Chen Q, Sun L, Chen ZJ. 2016. Regulation and function of the cGAS-STING pathway of cytosolic DNA sensing. Nat Immunol 17:1142–1149. https://doi.org/10.1038/ni.3558.
23. Fitzgerald KA, McWhirter SM, Faia KL, Rowe DC, Latz E, Golenbock DT, Coyle AJ, Liao SM, Maniatis T. 2003. IKKε and TBK1 are essential components of the IRF3 signaling pathway. Nat Immunol 4:491–496. https://doi.org/10.1038/ni921.
24. Lei CQ, Zhong B, Zhang Y, Zhang J, Wang S, Shu HB. 2010. Glycogen synthase kinase 3β regulates IRF3 transcription factor-mediated antiviral response via activation of the kinase TBK1. Immunity 33:878–889. https://doi.org/10.1016/j.immuni.2010.11.021.
25. Lin M, Zhao Z, Yang Z, Meng Q, Tan P, Xie W, Qin Y, Wang R, Cui J. 2016. USP38 inhibits type I interferon signaling by editing TBK1 ubiquitination through NLRP4 signalosome. Mol Cell 64:267–281. https://doi.org/10.1016/j.molcel.2016.08.029.
26. Ran Y, Zhang J, Liu L, Pan Z, Nie Y, Zhang H, Wang Y. 2016. Autoubiquitination of TRIM26 links TBK1 to NEMO in RLR-mediated innate antiviral immune response. J Mol Cell Biol 8:31–43. https://doi.org/10.1093/jmcb/mjv068.
27. Wang C, Chen T, Zhang J, Yang M, Li N, Xu X, Cao X. 2009. The E3 ubiquitin ligase Nrdp1 'preferentially' promotes TLR-mediated production of type I interferon. Nat Immunol 10:744–752. https://doi.org/10.1038/ni.1742.
28. Li S, Wang L, Berman M, Kong YY, Dorf ME. 2011. Mapping a dynamic innate immunity protein interaction network regulating type I interferon production. Immunity 35:426–440. https://doi.org/10.1016/j.immuni.2011.06.014.
29. Song G, Liu B, Li Z, Wu H, Wang P, Zhao K, Jiang G, Zhang L, Gao C. 2016. E3 ubiquitin ligase RNF128 promotes innate antiviral immunity through K63-linked ubiquitination of TBK1. Nat Immunol 17:1342–1351. https://doi.org/10.1038/ni.3588.
30. Zheng Q, Hou J, Zhou Y, Yang Y, Xie B, Cao X. 2015. Siglec1 suppresses antiviral innate immune response by inducing TBK1 degradation via the ubiquitin ligase TRIM27. Cell Res 25:1121–1136. https://doi.org/10.1038/cr.2015.108.
31. Cui J, Li Y, Zhu L, Liu D, Songyang Z, Wang HY, Wang RF. 2012. NLRP4 negatively regulates type I interferon signaling by targeting the kinase TBK1 for degradation via the ubiquitin ligase DTX4. Nat Immunol 13:387–395. https://doi.org/10.1038/ni.2239.
32. Zhang M, Wang L, Zhao X, Zhao K, Meng H, Zhao W, Gao C. 2012. TRAF-interacting protein (TRIP) negatively regulates IFN-β production and antiviral response by promoting proteasomal degradation of TANK-binding kinase 1. J Exp Med 209:1703–1711. https://doi.org/10.1084/jem.20120024.
33. Zhao Y, Liang L, Fan Y, Sun S, An L, Shi Z, Cheng J, Jia W, Sun W, Mori-Akiyama Y, Zhang H, Fu S, Yang J. 2012. PPM1B negatively regulates antiviral response via dephosphorylating TBK1. Cell Signal 24:2197–2204. https://doi.org/10.1016/j.cellsig.2012.06.017.
34. Huang J, Liu T, Xu LG, Chen D, Zhai Z, Shu HB. 2005. SIKE is an IKKε/TBK1-associated suppressor of TLR3- and virus-triggered IRF-3 activation pathways. EMBO J 24:4018–4028. https://doi.org/10.1038/sj.emboj.7600863.
35. Zhang K, Zhang Y, Xue J, Meng Q, Liu H, Bi C, Li C, Hu L, Yu H, Xiong T, Yang Y, Cui S, Bu Z, He X, Li J, Huang L, Weng C. 2019. DDX19 inhibits type I interferon production by disrupting TBK1-IKKε-IRF3 interactions and promoting TBK1 and IKKε degradation. Cell Rep 26:1258–1272. https://doi.org/10.1016/j.celrep.2019.01.029.
36. Mizushima N, Komatsu M. 2011. Autophagy: renovation of cells and tissues. Cell 147:728–741. https://doi.org/10.1016/j.cell.2011.10.026.
37. Yau R, Rape M. 2016. The increasing complexity of the ubiquitin code. Nat Cell Biol 18:579–586. https://doi.org/10.1038/ncb3358.
38. Bai L, Zhou H, Xu R, Zhao Y, Chinnaswamy K, McEachern D, Chen J, Yang CY, Liu Z, Wang M, Liu L, Jiang H, Wen B, Kumar P, Meagher JL, Sun D, Stuckey JA, Wang S. 2019. A potent and selective small-molecule degrader of STAT3 achieves complete tumor regression in vivo. Cancer Cell 36:498–511. https://doi.org/10.1016/j.ccell.2019.10.002.
39. Wang XJ, Yu J, Wong SH, Cheng AS, Chan FK, Ng SS, Cho CH, Sung JJ, Wu WK. 2013. A novel crosstalk between two major protein degradation systems: regulation of proteasomal activity by autophagy. Autophagy 9:1500–1508. https://doi.org/10.4161/auto.25573.
40. Mettenleiter TC. 2000. Aujeszky's disease (pseudorabies) virus: the virus and molecular pathogenesis: state of the art, June 1999. Vet Res 31:99–115. https://doi.org/10.1051/vetres:2000110.
41. Neumann CA, Krause DS, Carman CV, Das S, Dubey DP, Abraham JL, Bronson RT, Fujiwara Y, Orkin SH, Van Etten RA. 2003. Essential role for the peroxiredoxin Prdx1 in erythrocyte antioxidant defence and tumour suppression. Nature 424:561–565. https://doi.org/10.1038/nature01819.
42. Immenschuh S, Baumgart-Vogt E. 2005. Peroxiredoxins, oxidative stress, and cell proliferation. Antioxid Redox Signal 7:768–777. https://doi.org/10.1089/ars.2005.7.768.
43. Wood ZA, Schroder E, Robin HJ, Poole LB. 2003. Structure, mechanism and regulation of peroxiredoxins. Trends Biochem Sci 28:32–40. https://doi.org/10.1016/S0968-0004(02)00003-8.
44. Ishii T, Yamada M, Sato H, Matsue M, Taketani S, Nakayama K, Sugita Y, Bannai S. 1993. Cloning and characterization of a 23-kDa stress-induced mouse peritoneal macrophage protein. J Biol Chem 268:18633–18636. https://doi.org/10.1016/S0021-9258(17)46676-2.

45. Cao J, Schulte J, Knight A, Leslie NR, Zagozdzon A, Bronson R, Manevich Y, Beeson C, Neumann CA. 2009. Prdx1 inhibits tumorigenesis via regulating PTEN/AKT activity. EMBO J 28:1505–1517. https://doi.org/10.1038/emboj.2009.101.
46. Hoshino I, Matsubara H, Akutsu Y, Nishimori T, Yoneyama Y, Murakami K, Sakata H, Matsushita K, Ochiai T. 2007. Tumor suppressor Prdx1 is a prognostic factor in esophageal squamous cell carcinoma patients. Oncol Rep 18:867–871. https://doi.org/10.3892/or.18.4.867.
47. Shau H, Gupta RK, Golub SH. 1993. Identification of a natural killer enhancing factor (NKEF) from human erythroid cells. Cell Immunol 147:1–11. https://doi.org/10.1006/cimm.1993.1043.
48. Min Y, Kim MJ, Lee S, Chun E, Lee KY. 2018. Inhibition of TRAF6 ubiquitin-ligase activity by PRDX1 leads to inhibition of NFKB activation and autophagy activation. Autophagy 14:1347–1358. https://doi.org/10.1080/15548627.2018.1474995.
49. Wu J, Chen ZJ. 2014. Innate immune sensing and signaling of cytosolic nucleic acids. Annu Rev Immunol 32:461–488. https://doi.org/10.1146/annurev-immunol-032713-120156.
50. Helgason E, Phung QT, Dueber EC. 2013. Recent insights into the complexity of Tank-binding kinase 1 signaling networks: the emerging role of cellular localization in the activation and substrate specificity of TBK1. FEBS Lett 587:1230–1237. https://doi.org/10.1016/j.febslet.2013.01.059.
51. Tanaka M, Nishiyama Y, Sata T, Kawaguchi Y. 2005. The role of protein kinase activity expressed by the UL13 gene of herpes simplex virus 1: the activity is not essential for optimal expression of UL41 and ICP0. Virology 341:301–312. https://doi.org/10.1016/j.virol.2005.07.010.
52. Koyanagi N, Imai T, Shindo K, Sato A, Fujii W, Ichinohe T, Takemura N, Kakuta S, Uematsu S, Kiyono H, Maruzuru Y, Arii J, Kato A, Kawaguchi Y. 2017. Herpes simplex virus-1 evasion of $CD8^+$ T cell accumulation contributes to viral encephalitis. J Clin Invest 127:3784–3795. https://doi.org/10.1172/JCI92931.
53. Coulter LJ, Moss HW, Lang J, McGeoch DJ. 1993. A mutant of herpes simplex virus type 1 in which the UL13 protein kinase gene is disrupted. J Gen Virol 74:387–395. https://doi.org/10.1099/0022-1317-74-3-387.
54. Gu Z, Hou C, Sun H, Yang W, Dong J, Bai J, Jiang P. 2015. Emergence of highly virulent pseudorabies virus in southern China. Can J Vet Res 79:221–228.
55. Li L, Fan H, Song Z, Liu X, Bai J, Jiang P. 2019. Encephalomyocarditis virus 2C protein antagonizes interferon-β signaling pathway through interaction with MDA5. Antiviral Res 161:70–84. https://doi.org/10.1016/j.antiviral.2018.10.010.
56. Li L, Bai J, Fan H, Yan J, Li S, Jiang P. 2020. E2 ubiquitin-conjugating enzyme UBE2L6 promotes senecavirus A proliferation by stabilizing the viral RNA polymerase. PLoS Pathog 16:e1008970. https://doi.org/10.1371/journal.ppat.1008970.